10-2019

The Effect of Electromagnetic Fields Produced by WiFi Routers on the Magnetite (Fe3O4) Particles of the Italian Honey Bee (Apis mellifera ssp. ligustica)

Joseph Jungwirth
vr6815cy@go.minnstate.edu

The Effect of Electromagnetic Fields Produced by WiFi Routers on the Magnetite (Fe_3O_4) Particles of the Italian Honey Bee (*Apis mellifera* ssp. ligustica)

by

Joseph J. Jungwirth

A Thesis

Submitted to the Graduate Faculty of

St. Cloud State University

in Partial Fulfillment of the Requirements

for the Degree of

Master of Science

in Biology: Ecology/Natural Resources

October, 2019

Thesis Committee:
Matthew Julius, Chairperson
William Cook
John Sinko

Abstract

The Italian Honey Bee (*Apis mellifera* ssp. *ligustica*) is a commonly managed honey bee in the United States; however, two decades ago a decline in overwintering populations that led to a collapse of the population with no apparent cause had been observed. Past studies have shown that parasites (animal and viral) that infect the colony can lead to a collapse. In addition, neonicotinoid class pesticide exposure has been found to have a negative effect on the overall health of the hive and has led to colony collapses. Recently, a new idea has been proposed to be impacting bees physiologically: exposure to artificial electromagnetic fields. Honey bees possess nanoparticles within their abdomens composed of magnetite (Fe_3O_4), and they use these particles to detect the earth's electromagnetic field for orientation and thus navigation during foraging flights. Wireless fidelity (WiFi) routers at the 2.4 GHz frequency generate artificial magnetic fields which may pose a threat to the orientation of honey bees. A preliminary experiment was conducted to determine a method for extraction of magnetite nanoparticles and to verify the particles extracted were magnetic. A second in situ experiment was conducted to test the effect of a continuous electromagnetic field exposure at 2.4 GHz frequency would have on the magnetite particles produced by WiFi routers for 30 days. Results for the preliminary experiment show that the method of extraction is valid and that the particles extracted are indeed magnetic. Results for the second experiment suggest that exposure to 2.4 GHz waves for thirty days has no effect on the average particle size; in addition, the results suggest that there is no effect on the number of particles on average within individual honeybees post exposure.

Acknowledgements

First and foremost, I would like to thank my advisor Matthew Julius. I am appreciative of the fact that he took me on as a graduate student knowing that I would not be working with diatoms. I cannot thank you enough for the support that you have given me on this journey, and without your expertise of methodology and microscopy I would have been lost. I would also like to thank my committee members, William Cook and John Sinko. Cook's insights on statistical tests were detailed and helpful. Sinko's resources on RF radiation and knowledge about the Dynamic Light Scattering instrument was much appreciated, and without it my understanding would be far less than it is.

Next, I would like to thank the members and leaders of the Tri-County Bee Keepers Association of Stearns, Sherburne and Benton counties in St. Cloud, Minnesota. Without their knowledge of beekeeping and where to purchase supplies and live bees, I would not have been able to establish a new honey bee colony for experimentation.

Lastly, I would like to say a special "thank you" to all my friends and family who have supported me throughout the last three years while I have been working on my research. Without all of you it would not have been possible to make it to the end. A special thanks to Joshua Tacker for taking all of the photographs throughout the project despite not owning and therefore not wearing any protective gear.

Finally, I would like to thank my parents for the support and encouragement that they provided to me during this chapter of my life.

Table of Contents

Chapter Page

List of Tables

List of Figures

Chapter I: Introduction

Introduction

Insects make up much of the animal life on earth and together an entire class (insecta) of organisms that originated about 480 million years ago (mya) around the time of terrestrial plants in the Ordovician. The first group of terrestrial insects were land bound, but around 400 million years ago in the Devonian period, a lineage of insects evolved wings for flight being among the first to do so (Bradley et al., 2009). Global climate underwent several changes during the history of the Earth and with it the diversity of insects, as well. The winged insects (pterygotes) underwent a major radiation during the carboniferous (350-300 mya) period. Endopterygota (holometabola) underwent another major radiation during the Permian (299- 250 mya) period (Bradley et al., 2009). Most extant orders of insects developed during the Permian; however, many of these earlier groups became extinct during the Permo-Triassic boundary, known as the largest extinction event in history. Following the mass extinction event, several highly successful insect orders such as Hymenoptera (Bees, Wasps and Termites), Coleoptera (Beetles), Lepidoptera (Moths and Butterflies), and Diptera (Flies) co-evolved with flowering plants during the Cretaceous (145- 66 mya) period. Many of today's insect genera developed during the Caenozoic (66 mya) period.

Insect Development and External Anatomy

Apterygote (wingless) insects develop to adulthood with little change in body form (ametaboly), except for sexual maturation through development of gonads and genitalia. All other insects either have a gradual change in body form (hemimetaboly),

with external wing buds getting larger at each moult, or an abrupt change from a wingless immature insect to a fully mature winged adult form via a pupal stage (holometaboly). Immature stages of hemimetabolous insects are referred to as nymphs while holometabolous insects are referred to as larvae.

The external anatomy of insects is in general very similar with some variations. A key contributor to the success of the class insecta can be attributed to the cuticle. This inert layer provides internal support for the strong exoskeleton of the body and limbs and for muscle attachments. In addition, it acts as a barrier between living tissue and the outside environment. Internally, the cuticle lines tracheal tubes (breathing apparatus), gland ducts, and the foregut and hindgut of the digestive tract. The cuticle can range from rigid and armour-like, as in most adult coleoptera (beetles), to thin and flexible as in many larvae. However, one of the most crucial roles of the cuticle is the prevention of desiccation and the cuticle was necessary for the success of insects on land. Moreover, a vital role of the cuticle is that it is responsible for the varying cuticular extensions on the outside of an insect's body, varying from fine hair-like to robust spine-like protuberances. In adult and nymphal insects one of the most profound external features is the combination of segments into functional units, known as tagmosis. This process gave rise to the familiar tagmata or regions of an insect body known as the head, thorax and abdomen.

The head comprising of six segments generally consisting of antennae, light sensing organs referred to as occeli, eyes (in most cases), and a mouth with varying modifications among differing orders. The thorax consists of three segments (prothorax,

mesothorax and metathorax). The second segment has the wings along with the required musculature attached to it. Almost all adult insects possess three pairs of thoracic legs (one pair per segment) and these are typically used for walking, however, various other functions and modifications occur. An additional feature of the thorax is openings (spiracles) for gas-exchange and this tracheal system is present laterally on the second and third thoracic segments. Although, primitively, the abdomen possessed eleven segments, segment one may be reduced or fused into the thorax as is the case in many hymenoptera. Furthermore, the terminal segments can be variously modified or diminished. In general, the first seven segments of adult insects are similar in structure and lack any appendages. However, apterygotes and many immature aquatic insects possess rudimentary abdominal appendages called styles. An additional feature present on the abdomen is spiracles for gas exchange and typically are present on segments one through eight, but reductions in number can occur due to variations of the tracheal system. The anal-genital part of the abdomen known as the terminalia, generally consists of segments eight or nine to the abdominal apex. Segments eight and nine bear the genitalia for reproduction. Modifications can occur with segments ten and eleven and cerci or a pair of appendages may be present on segment eleven.

Insect Internal Anatomy

Members of the class insecta all possess a generalized form of internal anatomy with some variations or specializations present throughout the class among individuals. The insect body cavity called the haemocoel is filled with fluid (insect “blood”) called haemolymph and is lined with endoderm and ectoderm. Haemolymph washes over all

internal organs thereby delivering nutrients, and it also removes metabolites and conducts immune functions. However, haemolymph does not contain respiratory pigments and therefore does not play a role in gas-exchange like that of vertebrate blood. This function is performed by the tracheal system, a network of air filled tubes with finely branching extensions throughout the body. Non-gaseous waste is filtered from the haemolymph by finely branching tubules with free ends distributed throughout the haemocoel called Malpighian tubules. Their contents are emptied into the gut and after further modification, wastes are evacuated through the anus.

In most insects, the fat body is a perceptible internal component, usually forming a white-ish tissue comprising sheets, ribbons or lobes of cells within the haemocoel. The structure of this organ is taxonomically variable and underdefined. The fat body has many metabolic functions, such as the metabolism of carbohydrates, lipids, and nitrogenous compounds. In addition, it stores glycogen, fat, and protein, and it synthesizes major haemolymph proteins. The main cell type found in the fat body system is the trophocyte; this cell is responsible principally for most metabolic and storage functions mentioned above.

Insect Food Types and Gut Anatomy

Insects of different groups consume a variety of food types and specialization of the gut anatomy occurs depending on the physical characteristics of the food that an insect is consuming. For example, an insect that consumes solid food such as leaves or stems typically possess a wide, straight, and short gut with strong musculature and protection from abrasion. In contrast, an insect that consumes liquid food such as

phloem, nectar or haemolymph from other insects usually have a long, narrow and convoluted gut to allow maximal contact with food and thus maximum absorption of nutrients.

The generalized structure of an insect gut contains three main regions with sphincters controlling food-fluid movement between them. The three main regions of an insect gut are the foregut, midgut and hindgut. The foregut is responsible for ingestion, grinding, and transporting consumables to the midgut. In the midgut, enzymes for digestion are produced and released, and this is where absorption of nutrients and other digestive products takes place. Any remaining material left in the gut lumen along with any urine from the Malpighian tubules then enters the hindgut. In the hindgut, excess water, salts, and other valuable molecules are absorbed prior to evacuation of the feces through the anus. Areas of the gut display local specializations, which can be variably developed in insects depending on the food ingested. Generally, the foregut is subdivided into a pharynx, an oesophagus and a food storage area called the crop. In a forager honey bee, the crop is used as a nectar storage area (honey stomach) until it gets back to the colony for the dehydration process and storage of the nectar.

European Honey Bee

Honey Bees are a part of the class insecta in the order Hymenoptera, which also includes wasps, termites and ants. The hymenopteran order consists of about 105,000 species around the world with about 16,300 species in North America. The European honey bee (*Apis mellifera* L.) belongs to the family Apidae, consisting of around 25,000 species and is a part of the genus *Apis*. Honey bees such as *A. mellifera* L. are not

native to North America and were introduced in the 1600's from Europe for honey and wax production. Subspecies such as the Italian honey bee (*Apis mellifera* ssp. *ligustica*) were introduced in 1859 and other subspecies later from Spain, Germany and elsewhere (Agricultural Communications, 2006). Honey bees today are revered for their pollination efforts of garden crop produce and agricultural crop produce. An absence of honey bees would lead to a dramatically lower production yield. Honey bees contribute not only to the ecological realm by cross pollination of flowering plants but also to the economy from the production and sale of products such as wax, propolis, royal jelly and honey. Moreover, it is estimated that honey bees contribute $14 billion dollars annually to the United States economy (Calderone, 2012) with increased estimates worldwide.

Colony Collapse Disorder (CCD)

A decline in overwintering honey bee populations has been seen since early 2006. This phenomenon has been coined colony collapse disorder (CCD). It is characterized by the sudden, rapid, and mysterious disappearance of an entire colony's worker population. The workers abandon the queen, healthy brood, honey, and pollen stores without any visible cause. Without worker bees to replenish food stores in the hive the colony becomes unsustainable and it collapses (Oldroyd, 2007). Many hypotheses have been proposed to explain CCD such as ectoparasites like *Verroa destructor* mites (Donzé, Fluri & Imdorf, 1998), and tracheal mites such as *Acarapis woodi* (Johnson, 2007).

Another hypothesis posited to explain CCD are microsporidian gut parasites like *Nosema* Spp. (Oldroyd, 2007). Viral infections have been posited as well to explain

CCD such as, acute bee paralysis virus (ABPV) (Bailey, Gibbs, & Woods, 1963), deformed wing virus (DWV) (De Miranda & Genersch, 2010), and Israeli acute paralysis virus (IAPV) (Chen & Evans, 2007). Additionally, nutritional stress through habitat loss has also been proposed to be a factor leading to colony collapse disorder (Naug, 2009). Finally, pesticide exposure, to neonicotinoids, has also been looked at as a possible cause (Lu, Warchol, & Callahan, 2014).

Honey Bee Orientation

In the past two decades, efforts have been made to study another possible cause of bee losses and subsequently a contributor to CCD: anthropogenic electromagnetic fields emitted by devices such as wireless fidelity (WiFi) routers. Honey bees orientate themselves in their environment by using a multitude of behavioral mechanisms and environmental cues. These are organized hierarchically: a primary system consisting of an environmental cue (The Sun) and a backup system that is relied on when the primary cue is absent or not readily available (Dyer & Gould, 1983).

In order for honey bees to utilize the sun as a cue for orientation and thus navigation, they must be able to compensate for its movement westward with the passage of time. Honey Bees use the Sun's azimuth, its compass direction in relation to north, designated 0°, as their reference for orientation and they learn the Sun's azimuthal movement during their first flight (Dyer & Gould, 1983). Polarized ultraviolet light is another orientation cue relied on in the primary system as long as there is a patch of blue sky available. This polarized light is utilized to infer the Sun's position and hence the bee's position for orientation (Dyer & Gould, 1983). However, it is known that

polarized light cannot penetrate full cloud cover and thus honey bees must possess a secondary system of environmental cues to rely on when there are days of uninterrupted cloud cover.

One of those cues is the reliance on fixed positional objects or landmarks in order to determine the Sun's position on cloudy days by resorting to a memory of the Sun in relation to the surrounding fixed objects near the hive (Dyer & Gould, 1983). It is also understandable that a further back up system is needed when fixed objects are unreliable; therefore, a ternary cue that is thought to be relied on when the Sun and fixed objects are not present is the Earth's magnetic field. However, there has been very little research conducted on the Earth's magnetic field and its utilization for an orientation mechanism by honeybees.

Previous Magnetic Field Exposure Effects

Honey bees show four variable effects when exposed to electromagnetic fields (EMF) (Gould, Kirschvink, Deffeyes, 1978). The first of these that was discovered was that during a honey bee's waggle dance, while converting the angle flown to a food source in relation to both the Sun and gravity, they make small regular errors related to the dance and the Earth's magnetic field. When the magnetic field is cancelled, the errors disappear (Gould et al., 1978). A second effect discovered was that when the bee's honeycomb is turned on its side, bees are forced to dance horizontally, which deprives them of their gravity cue; as a result some will stop dancing and others will dance in a disorienting fashion. Nonetheless, after a couple of weeks, the disoriented bees will reorient themselves to the four cardinal points of the magnetic compass.

Nevertheless, cancelling the Earth's magnetic field stops this reorientation (Gould et al., 1978). A third effect due to magnetic exposure that was found, is that when a swarm of honeybees is placed in a cylindrical hive, being completely deprived of all orientation cues, the swarm builds its comb in the same magnetic direction as the parent hive, eluding to a form of magnetic memory (Gould et al., 1978). Lastly, the fourth effect that was found is that when honey bees are deprived of all orientation cues, their circadian rhythms are set to the daily variations of the Earth's electromagnetic field; yet these rhythms are disrupted when an abnormally strong field is applied (Gould et al., 1978).

With the previous findings it is plausible that honeybees have magnetic detectors used for magnetoreception of the Earth's EMF, which can be measured by the bee's nervous system. Gould et al. (1978), determined that honey bees exhibit natural remanence with a preferred direction and no tendency to track an applied field. Furthermore, Gould et al. (1978), also found that the source of this magnetism and thus magnetic material was located in the anterior portion of the abdomen and could be suitable to be used as a detector. He also cited that a honey bee would need to build many single magnetic domains and space them apart so they do not interact and cancel each other's field.

Magnetic Particles

Through iron depositing vesicles (IDV), honey bees deposit iron minerals intracellularly within trophocytes which are located in the anterior portion of the abdomen. Here, iron granules are formed, randomly distributed, and mature 25 days after eclosion (Hsu & Li, 1993). Magnetite crystal (Fe_3O_4) structures are found within the

iron granules and the iron granules possess an average diameter of 0.5 ±0.1 microns (Hsu & Li, 1994). Hsu and Li (1994) indicated that if the observed magnetite crystals are indeed used for magneto reception, then innervation of the trophocytes to the nervous system must exist.

In fact, the trophocytes were found to be innervated to the nervous system thus lending to the idea that these crystals are used for magneto-reception (Hsu & Li, 1994). It was also suggested that external magnetic fields may cause an expansion or contraction of the iron granules depending on their orientation (Hsu & Li, 1994). To follow up, Hsu, Ko, Li, Fann, & Lue (2007) later determined that an additional magnetic field (1 Gauss) applied to live trophocytes for two minutes induced a size change in iron granules. The results demonstrated that iron granules shrank 12±1.7% at the paralleled direction to the magnetic field and enlarged 1.2±0.5% at the vertical direction in the horizontal plane (Hsu et al., 2007).

Magnetoreception

The four previous studies have mainly focused on the location and formation of the iron granules and have indicated that the iron granules possess the ability to be magneto-receptors. However, they have not directly related iron granules with the honey bees' ability to perceive magnetic fields. A study conducted by Liang, Chuang, Jiang, & Yang (2016), using classical conditioning, trained honey bees to associate a magnetic stimulus with the proboscis extension reflex (PER), resulting in an extension of their proboscis when a magnetic stimulus is present. Once the authors cut the ventral nervous cord, the connection from the brain to the rest of the body, they found that PER

stopped when a magnetic stimulus was present, thereby, confirming evidence of an association of iron granules with magnetoreception (Liang et al., 2016). Considering the results mentioned thus far, it can be inferred that honey bees receive magnetic information and it is most likely from the iron granules located in their abdomens.

Past RF Wave Exposure Studies

Headlee and Burdette (1929) found that *Apis mellifera* L. die due to a lethal internal increase in temperature (ranging from 110.1 to 124.5 °F in the thorax and from 101.4 to 111.2 °F in the abdomen) and temperatures increase at higher rates in insects with highly specialized nervous tissue after being exposed to radio waves at a frequency of 12 megahertz (MHz). A study conducted by Sainudeen (2011) found that after exposure to a cell phone frequency of 900 MHz, worker bees elicited a behavior change and never returned to the test hives. Additionally, bee strength (number of honey-filled frames) was significantly lower in the test hives compared to the control hives. Furthermore, queens produced significantly less eggs per day in the test hives compared to the control hives. A related study found that exposure to a cell phone frequency of 900 MHz elicited physiological changes in *A. mellifera* L. ssp. ligustica such as a significant decrease in carbohydrate, lipid and protein concentrations following a 40-minute exposure (Kumar, Sangwan & Badotra, 2011). The previous studies showcase evidence of a physiological effect elicited by exposure from RF radiation at a low frequency, however, the past decade has seen an increase in frequencies and power used for wireless communication such as wireless routers.

Wireless Fidelity (WiFi)

Increased interest in municipal wireless connections has occurred since 2005, mainly due to the increased prevalence of portable devices (Jassem, 2010). Municipal systems would be able to move some government functions online thereby increasing access to the government and enticing more participation of the city's residents in government processes. In the United States, the most commonly used Industrial-Scientific-Medical (ISM) band of frequency emits in the 2.4-2.5 GHz range, and it is most often used by wireless devices for connecting to the internet through WiFi routers (Gast, 2005). The first major cities to implement a city wide WiFi system were Philadelphia in 2005 and San Francisco two years later, followed by many more cities implementing their own infrastructures in the following years (Jassem, 2010). Wireless Fidelity router infrastructures are not the only environmentally relevant EMF exposure hazards that honey bees face but they are weaker in terms of power level and magnetic field strength when compared to others (Table 1.1).

Table 1.1. Environmentally relevant electromagnetic field exposure hazard sources to *Apis mellifera* ssp. ligustica with corresponding average radiated power output and calculated magnetic field intensity.

Source	Average Radiated Power (P) (Watts)	Magnetic Field Intensity (B) (Gauss)****
Wireless (WiFi) Network Router*	0.003*	5.01×10^{-5}
Cellular Phones	0.3**	5.01×10^{-4}
Car Radio	45**	6.14×10^{-3}
Cellular Broadcast Tower	100**	9.15×10^{-3}
Radio Broadcast Towers	2000000**	1.29
Power Lines	765000000***	25.3

*Power level and source used for this study.

**Zamanian, A., & Hardiman, C. (2005). Electromagnetic radiation and human health: A review of sources and effects. *High Frequency Electronics*, *4*(3), 16-26.

***Tenforde, T. S. (1992). Biological interactions and potential health effects of extremely-low-frequency magnetic fields from power lines and other common sources. *Annual Review of Public Health*, *13*(1), 173-196.

****Lorrain, P., & Corson, D. R. (1970). Electromagnetic fields and waves. *Electromagnetic fields and waves., by Lorrain, P.; Corson, DR. Second edition. San Francisco, CA (USA): WH Freeman, pp.402-405.*

Chapter II: Preliminary Experimentation

Study Objectives. A preliminary experiment was conducted to:

1. Create a method of extraction for the retrieval of the magnetite nanoparticles from within a honey bee abdomen.

2. Validate the extraction of the particles, confirm that they are magnetic, and verify the instrument used is able to detect and measure the extracted particles.

Methods

Honeybees. A standard 10-frame Langstroth hive was set up in the overflow parking area of Q-Lot at Saint Cloud State University in St. Cloud, Minnesota. A sucrose solution (1:1 ratio) was added to the hive during the early weeks of spring (2017) as a dietary supplement until the first nectiferous flower bloom began. Four honeybees, 25-35 days after egg eclosion, were randomly selected. Age was controlled for by monitoring egg clutches that were laid by the queen, and this information was recorded on the brood frames.

Passivation. Iron will not dissolve in highly concentrated nitric acid (HNO_3) due to a chemical property known as passivation. Reaction of surface iron with concentrated acid forms a metal-oxide layer that protects a bulk of the metal from being oxidized. Due to this property of HNO_3, 68-70% concentrated nitric acid was used to dissolve the organic tissue of individual honey bee abdomens.

Magnetic particle extraction. Honey bees were cold euthanized. Their abdomens (N=4) were dissected. The abdomens were then placed into a 250 mL glass beaker. Ten milliliters of 68-70% concentrated HNO_3 was added to the beaker. A watch

glass was placed over the beaker. The beaker was placed onto a hot plate on a very low heat setting. The hot plate and beaker were then placed under a fume hood overnight, after which time the sample was then poured into a 50 mL conical test tube. The test tube was filled with deionized water (DI). The test tube was placed into a centrifuge. The test tube was spun at 4000 rpm at 25 °C for 10 minutes to force the iron granules to the bottom. The supernatant was aspirated down to an amount of 1.5 mL. The test tube was refilled with DI water, and centrifuged again. The three above sample wash steps of refill, centrifuge and aspiration were repeated for a total of three times. The final 1.5 mL sample was placed into a cuvette for analysis.

Magnetic particle verification. To verify that the particles that were extracted were magnetic, the sample obtained was first, measured using a Malvern Zetasizer Nano ZS dynamic light scattering (DLS) instrument (Figure 1.2) and an average particle size was obtained. Next, a micro-magnetic stir bar was placed into the sample with the idea being that the magnetic stir bar would attract and therefore remove any magnetic particles from the sample. The sample was placed onto a magnetic stir plate (Figure 2.2) and allowed to stir slowly for 5 hours. After which time it was again analyzed using the DLS instrument. An average particle size was obtained from the DLS.

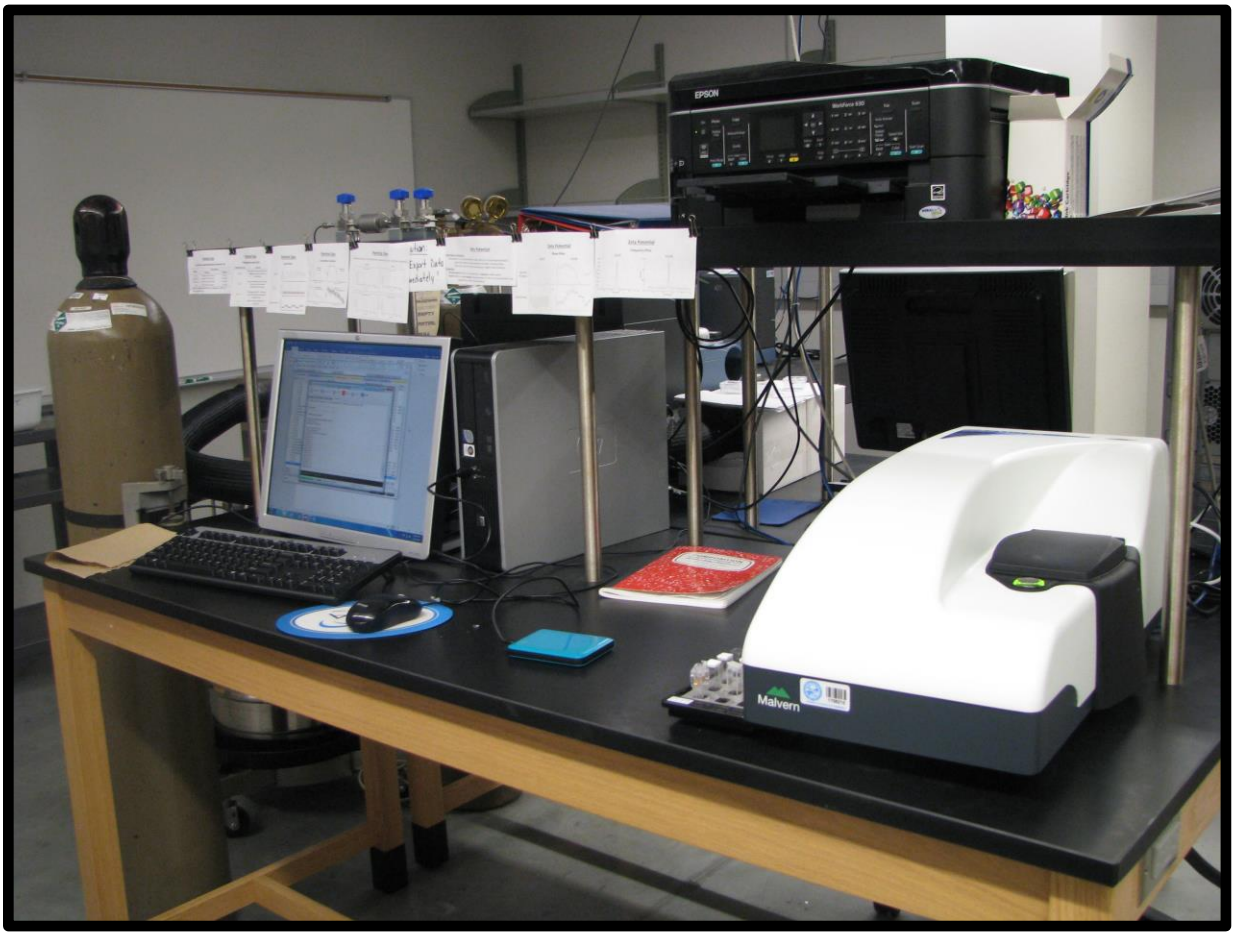

Figure 1.2. Dynamic Light Scattering instrument used for magnetic particle verification and average magnetite (Fe_3O_4) particle size analysis.

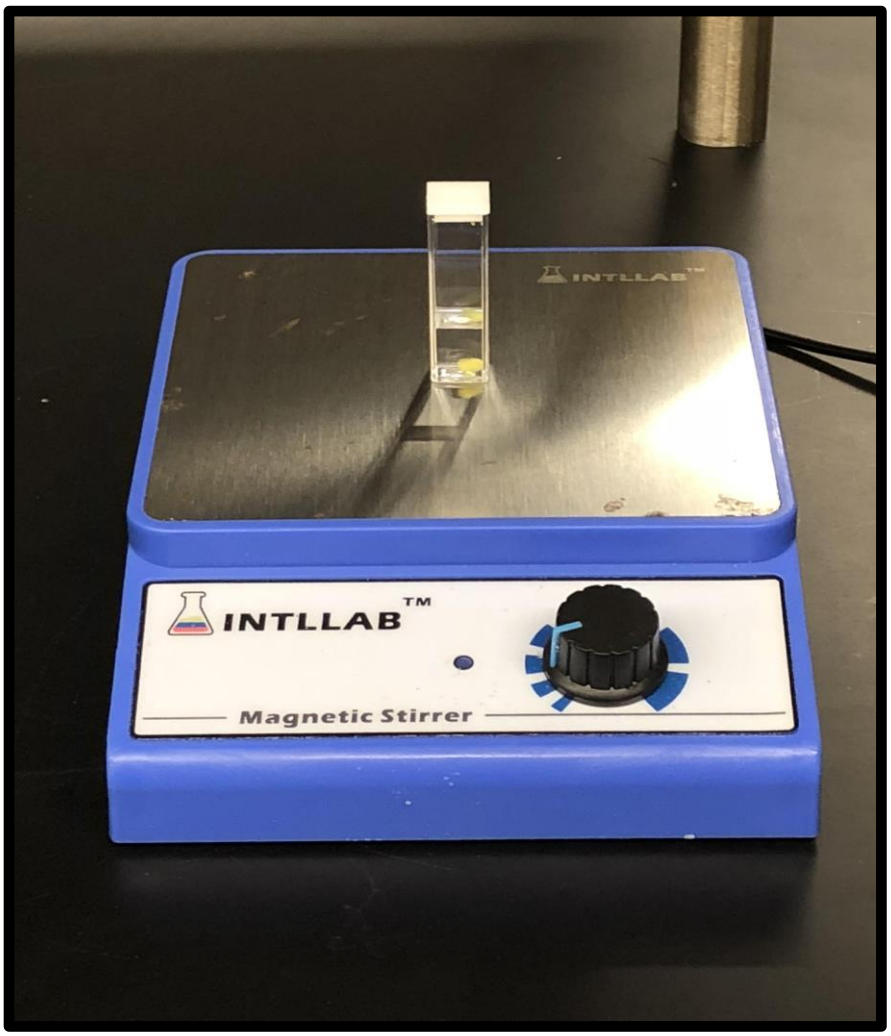

Figure 2.2. Preliminary experiment sample with micro stir bar; resting on the magnetic stir plate utilized for the 5 hour magnetic stirring event.

Results

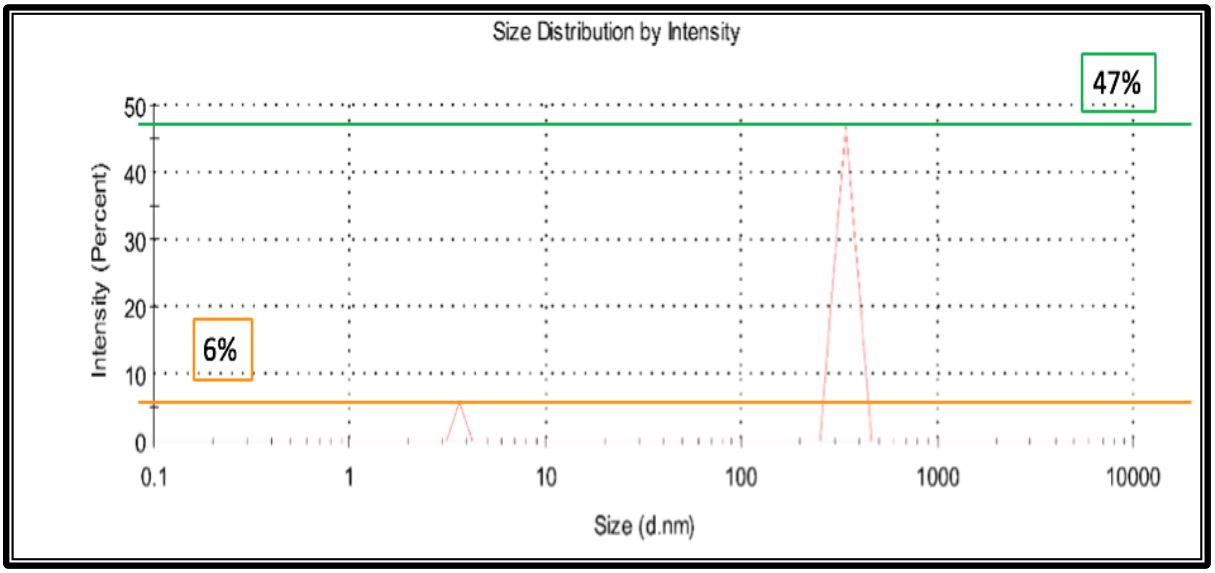

Figure 3.2. Dynamic light scattering instrument size analysis results prior to a 5 hour magnetic stirring event.

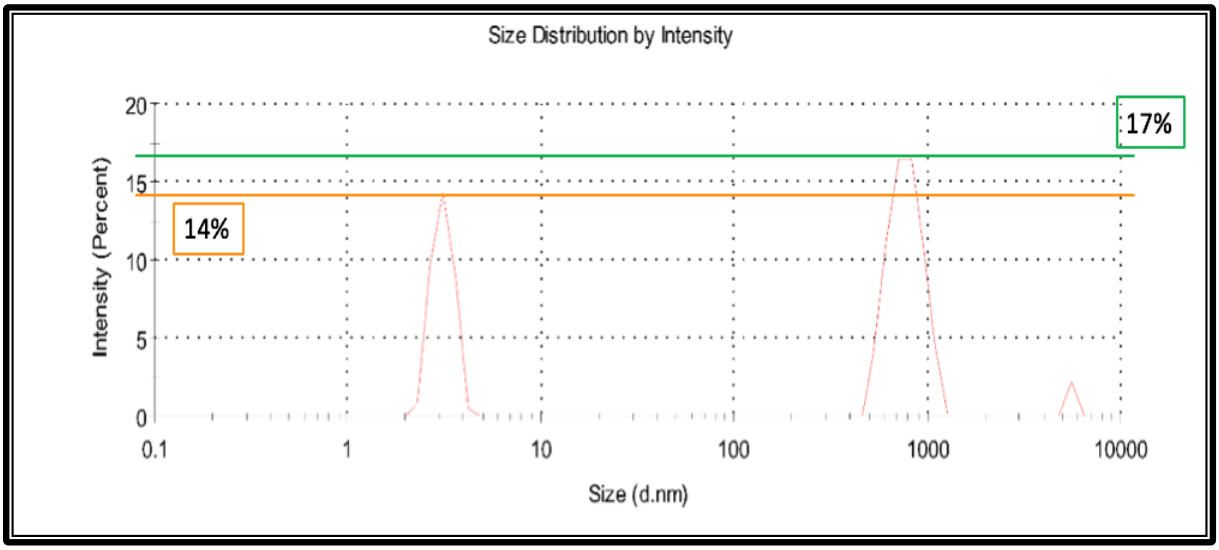

Figure 4.2. Dynamic light scattering instrument size analysis results after a 5 hour magnetic event.

Preliminary data. Results for the preliminary experiment present two particle size averages with values of 3.123 nm (SD= 0.3348 nm) and 343.4 nm (SD= 104.6 nm). Results also show corresponding particle intensity (percentage) values of 6% and 47%, respectively, prior to a magnetic stirring event (Figure 3.2). Following a magnetic stirring event, results showcase three average particle sizes of 3.123 nm (SD= 0.3821 nm), 783.6 nm (SD= 152 nm) and 5,560 nm. Moreover, corresponding particle intensity values of 14% and 17%, for the first two average particle sizes were also found (Figure 4.2).

Discussion

Following the magnetic stirring event, the average particle size peak of 3.123 nm did not disappear nor did it change in average size. This result confirms that the first of the two average particle sizes shown in figure 3.2 are impurities or dust or at the very least not magnetic. These impurities were found within the facility's deionized water system, supported through subsequent analyses of ultrapure water versus deionized water using the DLS. The second average particle size distribution shown is within the average size range of 0.5 microns that has been reported in previous literature for the magnetic particles found within *A. meliffera* L. ssp. *ligustica* used for magneto reception (Hsu & Li, 1994). Therefore, these particles are the subject of investigation. After the magnetic stirring event occurred, analysis with the DLS instrument yielded results of three average particle size peaks (Figure 4.2). The first of three is the same average particle size as the first peak in figure 3.2, with a notable change in particle intensity, increasing from 6% to 14%. The second average particle size peak has increased from 343.4 nm to 783.6 nm with a notable decrease in particle intensity from 47% down to 17%. The third average particle size peak of 5,560 nm originates from the micro stir bar that was placed into the sample and could be due to surface scattering of the stir bar.

Results were validated due to the fact that the average particle size peak under investigation increased in average size and decreased in particle intensity after the magnetic stirring event. This occurred due to the magnetic micro stir bar attracting and removing the smaller particles in the sample. This decrease in the number of target particles within the sample led to the decrease of particle intensity and thus to a ratio

change. Therefore, the decrease in particle intensity allowed more of the non-target particles in the sample to be more heavily weighted in the analysis (Figure 4.2). Hence, these preliminary results confirm the presence of magnetic particles within *A. mellifera* ssp. *ligustica* and validate the extraction method utilized.

Chapter III: Full Hive Continuous Exposure Experiment

Rationale

Previous studies showcase physiological effects in the honey bee from frequencies of 12 and 900 MHz. Moreover, an exposure to a magnetic field induced a size change effect of magnetic particles within *A. mellifera* (Hsu et al., 2007). Due to an undeniable increase in the prevalence of WiFi routers that generate artificial electromagnetic fields, a 30 day continuous exposure experiment was set up to test the effect that exposure to 2.4 GHz frequency EMF had on the size and abundance of magnetite particles within *A. mellifera* L. ssp. ligustica.

Hypotheses

Since previous studies showcased a physiological effect after exposure to artificial electromagnetic fields from cellular phones, and an increase of WiFi routers can be observed, two hypotheses were formulated:

- Continuous exposure to an artificial electromagnetic field (2.4 GHz frequency) will induce a size change of magnetic particles in *A. mellifera* L. spp. ligustica.
- Continuous exposure to an artificial electromagnetic field (2.4 GHz frequency) will induce an abundance change of magnetic particles in *A. mellifera* L. spp. ligustica.

Methods

Honey bees. A standard 10-frame Langstroth honey bee (*Apis mellifera* L. ssp. ligustica) hive was set up on April 27, 2018 in the parking area of Q lot at Saint Cloud State University in St. Cloud, Minnesota. A sucrose solution (1:1 ratio) was added to the

hive during the early weeks of spring as a dietary supplement until the first nectiferous flower bloom began.

High frequency radiation exposure. A Hewlett Packard E4433B digital RF Signal Generator (250 kHz- 4 GHz) with a 3 milliwatt (mW) power output level was utilized for the 2.4 GHz frequency artificial electromagnetic field exposure (Figure 5.3). The full hive exposure started on August 15, 2018 at 4 o'clock post-meridian (pm) time. The hive was continuously exposed for 30 days. The exposure ended on September 14, 2018 at 4 o'clock pm time. During the thirty day continuous exposure, the whole hive was surrounded by a 1.5 centimeter square shaped chicken wire fence to act as a Faraday cage in order to mitigate any unwanted exposure to surrounding persons or animals (Figure 6.3).

Figure 5.3. Hewlett Packard E4433B digital RF Signal Generator (250 kHz- 4 GHz) with 2.4 GHz rubber ducky antenna attached. Unit is housed within a pine box for weather protection during 30 day continuous exposure.

Figure 6.3. Experimental hive surrounded by (1.5 cm diameter openings) a chicken wire fence to act as a Faraday cage to mitigate any harmful unwanted exposure to high frequency waves.

Sampling & data analysis. Twenty-five honey bees (25-35 days after egg eclosion) were randomly selected for the pre-exposure condition. Twenty-five honey bees (25-35 after eclosion) were randomly selected for the post-exposure condition. Age was controlled for by monitoring egg clutches, which were laid by the queen every two days, and by observing newly metamorphosed adults that were emerging from their brood cell. The age information was then recorded on the brood frames and in a field notebook for future reference. Differences between the study parameters of average

size (nm) and abundance were analyzed using a two-sample one-tailed T-test assuming unequal variances preliminarily in Microsoft Excel. For all statistical tests the differences were considered significant at p-value < 0.05.

Magnetic particle extraction. The honey bees were cold euthanized. The abdomens were excised. The abdomens were placed into 10mL of 70% concentrated nitric acid (HNO_3). The abdomens were then dissolved using a Mars 6 one-Touch™ microwave digestion system (Figure 7.3) using a pre-programmed animal tissue digestion standard operating procedure (see appendix A). Following the digestion of organic tissue, the solution was put through a series of sample washes by decanting the solution into a 50mL conical centrifuge tube. Forty milliliters of ultra-pure water was added to the centrifuge tube. The centrifuge tube was then spun in a centrifuge for 10 minutes at 4000 rpm at 25 °C to force the iron granules to the bottom of the tube. The supernatant was then aspirated down to an amount of 1.5 mL. The above steps were repeated for a total of three times. The final 1.5 mL volume solution was then analyzed using a Malvern Zetasizer Nano ZS dynamic light scattering (DLS) instrument. Finally, the average particle size was obtained for each of the 25 samples for both the pre-exposure and post-exposure conditions (see appendix B).

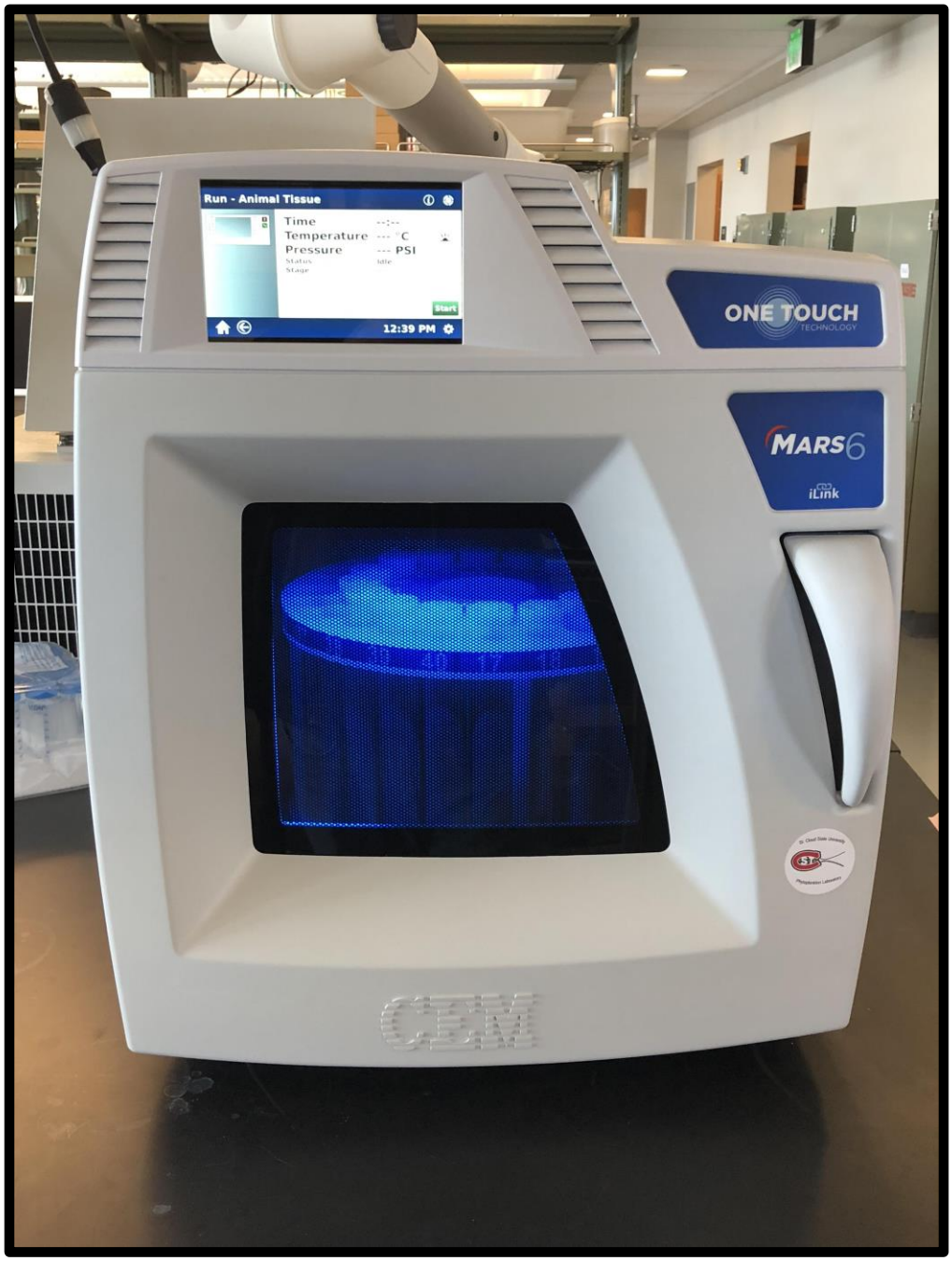

Figure 7.3. Mars 6 one-Touch™ microwave digestion system utilized for magnetite (Fe_3O_4) particle extraction with nitric acid (HNO_3).

Scanning electron microscopy. After DLS analysis, each sample from the pre-exposure and post-exposure conditions was placed into a 10 ml glass graduated cylinder. An N50 ½'' x ½'' cylindrical rare earth neodymium magnet with a strength of 1 Tesla was attached to the outside bottom of the graduated cylinder for magnetic particle purification (Figure 8.3). The samples were allowed to sit for 2 days. The supernatant was then decanted. Sixty microliters of ultrapure water was pipetted into the graduated cylinder. The magnet was removed. The sample was then allowed to rest for 10 minutes. After ten minutes, the 30 microliter sample was then pipetted onto a 9.0 mm carbon tape, which was attached to one side of a 9.5 mm x 9.5 mm aluminum specimen mount. The samples were then allowed to dry for 3 days under a 250 mL glass beaker (Figure 9.3).

Once dry, iron particles were counted for each sample using a JEOL JSM-6060LV scanning electron microscope (SEM) operating at an accelerated voltage of 15 kV, with a working distance of 10-15 mm (see appendix). The elemental composition of each particle was verified by using an energy dispersive X-ray spectrometer or EDS (Figure 10.3).

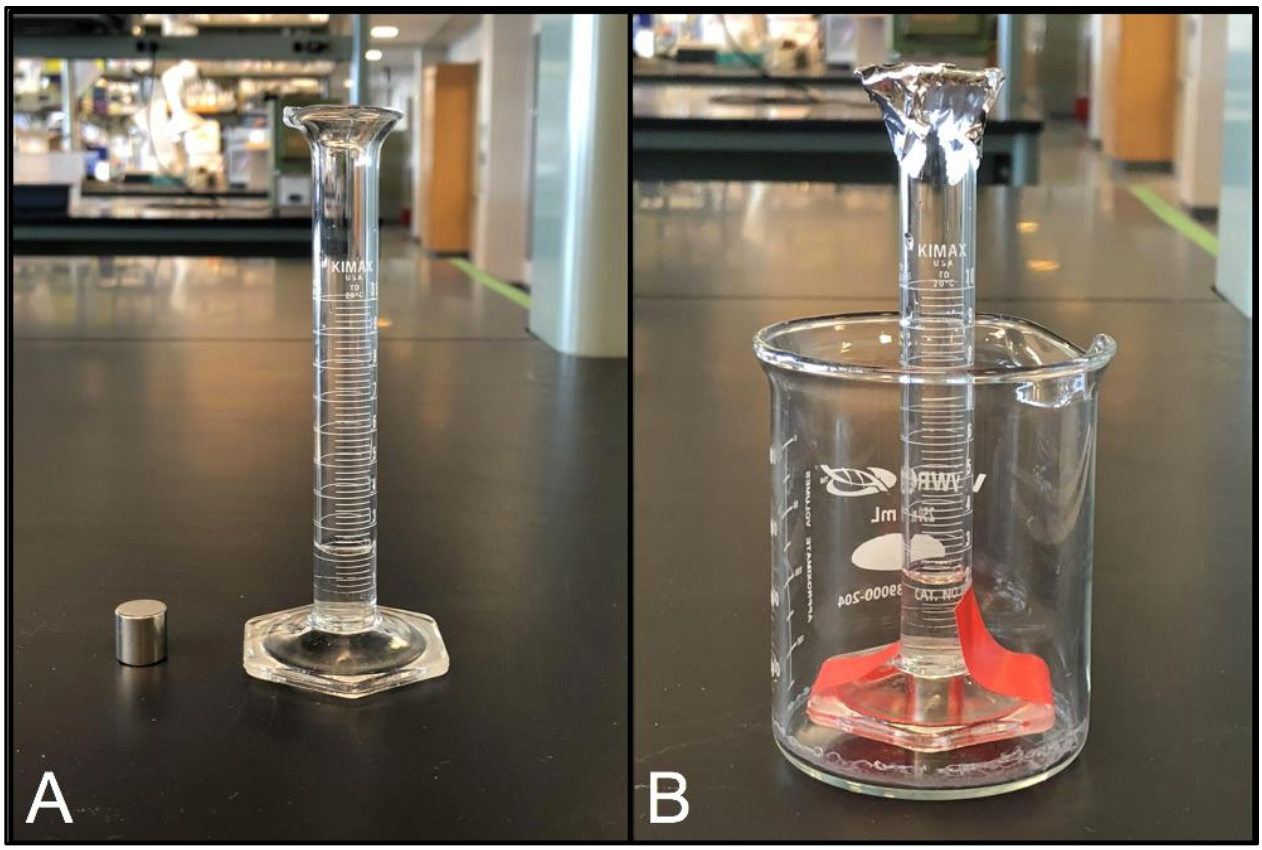

Figure 8.3. Apparatus setup for magnetite particle separation: A. 10 ml glass graduated cylinder with a N50 ½'' x ½'' rare earth neodymium 1 Tesla strength magnet. B. Magnet attached to bottom of graduated cylinder with aluminum foil cover while resting for 2 days.

Figure 9.3. Sample preparation for Scanning electron microscopy and energy dispersive X-ray spectrometry analysis.

Figure 10.3. Scanning electron microscope and energy dispersive X-ray spectrometer work station for particle abundance analysis.

Results

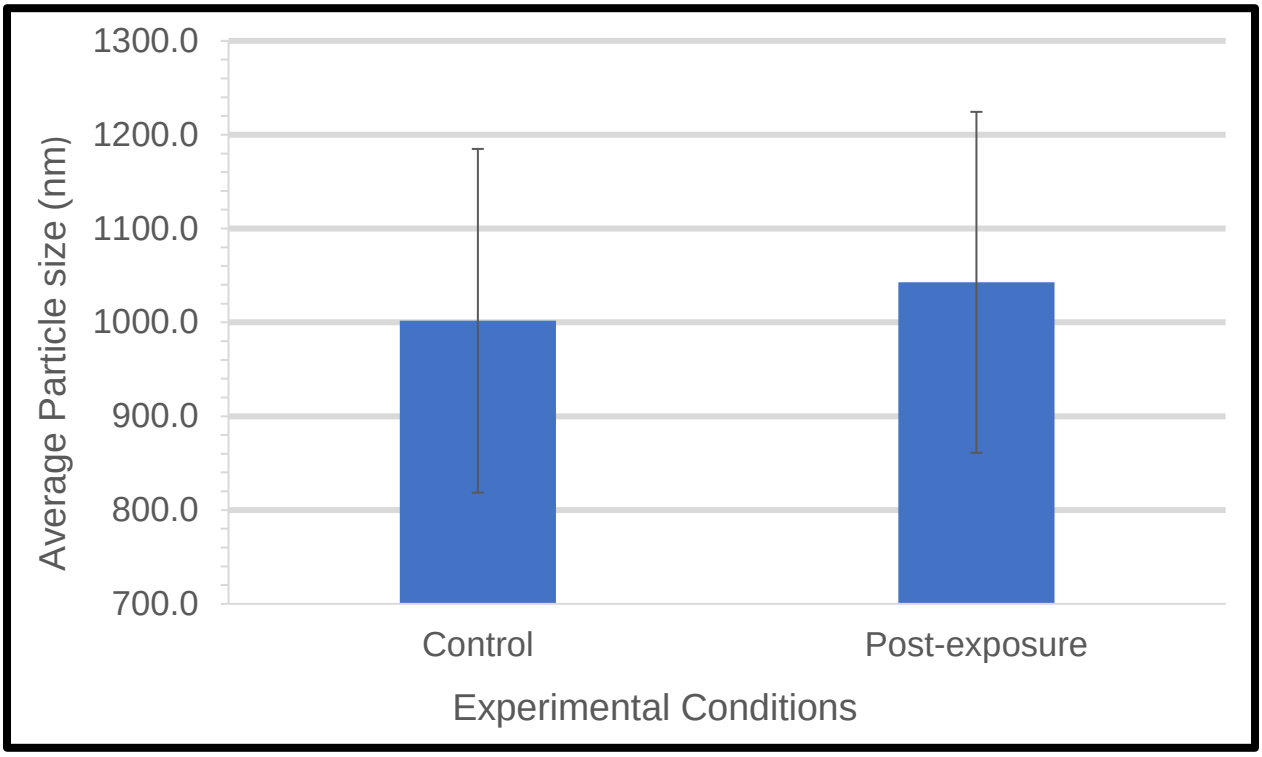

Figure 11.3. Magnetite particle average size results for pre and post 2.4 GHz high frequency wave exposure.

Particle size data. Prior to exposure from an artificial electromagnetic field at a frequency of 2.4 GHz, the average size of particles was found to be 1001.7 nm (SD=183.2 nm). Following a 30 day exposure, the average size of particles in the samples was found to be 1042.7 nm (SD=181.7 nm) (Figure 11.3). Statistical analysis of the pre-exposure average particle size (N=23) and of the post-exposure average particle size (N=25) indicated a non-significant difference between the pre-exposure and the post-exposure conditions (p-value= 0.22).

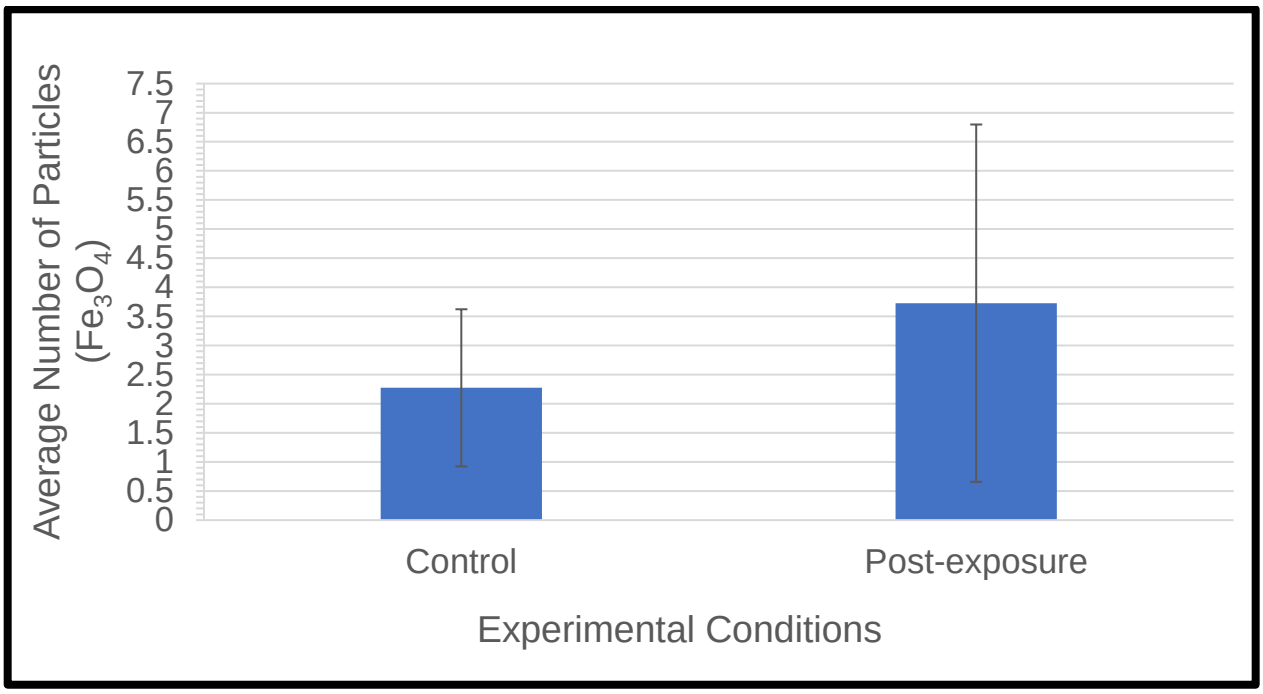

Figure 12.3. Magnetite particle average abundance results for pre and post 2.4 GHz high frequency wave exposure.

Particle abundance data. Prior to exposure, the average number of iron particles present within *A. mellifera* ssp. ligustica was found to be 2.27 particles (SD=1.35 particles). Following a 30 day exposure, the average number of particles was found to be 3.73 (SD=3.07 particles) (Figure 12.3). Statistical analysis of the pre-exposure average number of particles (N=11) and the post-exposure average number of particles (N=11) indicated a non-significant difference between the pre-exposure and the post-exposure conditions (p-value= 0.086).

Discussion

In this study, it was found that there was not a significant increase or decrease in the average size of magnetic particles after being exposed to an artificial

electromagnetic field at a frequency of 2.4 GHz. It was also found that the average size of particles within *A. mellifera* ssp. *ligustica* abdomens was not found to be 0.5 ±0.1 microns (Hsu & Li, 1994), but rather, the results show an average particle size of around 1 ±0.183 micron. This is counter to the results that were found by previous researchers looking at size changes of iron particles after being exposed to a magnetic field. These researchers found that the particles shrank 12±1.7% at the paralleled direction to the magnetic field and enlarged 1.2±0.5% at the vertical direction in the horizontal plane (Hsu et al., 2007). Not washing *A. mellifera* ssp. *ligustica* before dissection was a problem that could have occurred and contributed to the larger size measurement of magnetic particles. While analyzing with the SEM, a large number of silicon oxide or sand particles was found; therefore, this would have contributed to the average particle size analysis thus skewing it to the increased size direction rather than to the reported size of previous findings. Hence, with these results it can be concluded that there is not enough evidence to support the hypothesis that continuous exposure to an artificial electromagnetic field will induce a size change of magnetic particles within *A. mellifera* ssp. ligustica.

This study also found that there was not an increase statistically to the abundance of magnetic particles within *A. mellifera* ssp. *ligustica* abdomen after a continuous exposure to artificial electromagnetic fields emitted by WiFi routers. However, although there was not a statistically significant (p-value= 0.086) difference between the pre-exposure group and the post exposure group average number of particles, it is believed that a statistical significance could have been found between the

two groups' averages if the sample size were larger. The sample size can be increased with some modifications to the method of particle extraction. If a magnet is attached to the outside bottom of the microwave digestion tube after digestion, then the particles will be attracted to the bottom. Furthermore, if the nitric acid is removed from the sample instead of being placed into a conical test tube after digestion, it will allow for fewer sample rinses and fewer aspirations of the supernatant, which would lead to fewer particles being lost. Moreover, if the previous modifications were implemented, then the centrifuge step would not be needed, thereby reducing the amount of time needed for particle extraction. Although there was not a statistically significant difference of both average particle size and average particle counts found between the non-exposed and exposed experimental groups, a biological trend of an increase to the average size and average number of particles after being exposed was observed (Figures 11.3 & 12.3). This would indicate that while being subjected to additional magnetic fields a honey bee must develop more particles for the use of orientation in order to navigate itself back to the colony. However, with these results, it is concluded that there is not enough evidence to support my hypothesis that exposure to high frequency (2.4 GHz) artificial EMF pollution will induce an abundance change of magnetic particles in *A. mellifera* L. spp. ligustica. However, there is in my opinion enough evidence to support a trending result in the abundance change of particles within a honey bee abdomen after exposure and therefore I can safely say that the data is not statistically significant but is consistent with the hypothesis.

Chapter IV: Conclusion

A decline in honey bee populations has been observed for the last two decades with no definitive single cause identified. Past environmental pressures such as parasites (both fauna and viral) and nutritional stress due to habitat loss have been shown to negatively impact honey bee populations, leading to colony collapse, but are not the sole causes of the observed population declines. The non-statistical pattern observed in this study of an increase in the average size and average abundance of magnetic particles from exposure from WiFi router EMFs may just be another stressor impacting honey bee populations at a time when populations are already overstressed. Any population can remediate and adapt itself to a single stressor that is negatively impacting it; however, once multiple stressors start to add up, a synergistic effect could take place. At a certain point, those stressors impact a population at such a level that it is not sustainable and therefore could lead to a collapse of that population (Coors & De Meester, 2008). With that being said, more research must be conducted on WiFi router EMFs and their impact on biological organisms.

References

Bradley, T. J., Briscoe, A. D., Brady, S. G., Contreras, H. L., Danforth, B. N., Dudley, R., ... & Reppert, S. M. (2009). Episodes in insect evolution. *Integrative and Comparative Biology*, *49*(5), 590-606.

Bailey, L., Gibbs, A. J., & Woods, R. D. (1963). Two viruses from adult honey bees (Apis mellifera Linnaeus). *Virology*, *21*(3), 390-395.

Calderone, N.W. (2012). Insect pollinated crops, insect pollinators and US agriculture: trend analysis of aggregate data for the period 1992-2009. *PLoS ONE* 7(5).

Chen, Y., & Evans, J. D. (2007). Historical presence of Israeli acute paralysis virus in the United States. *American bee journal*, *147*(12), 1027-1028.

Coors, A., & De Meester, L. (2008). Synergistic, antagonistic and additive effects of multiple stressors: predation threat, parasitism and pesticide exposure in Daphnia magna. *Journal of Applied Ecology*, 45(6), 1820-1828.

De Miranda, J. R., & Genersch, E. (2010). Deformed wing virus. *Journal of invertebrate pathology*, *103*, S48-S61.

Dyer, F., & Gould, J. (1983). Honey Bee Navigation: The honey bee's ability to find its way depends on a hierarchy of sophisticated orientation mechanisms. *American Scientist*, 71(6), 587-597.

Donzé, G., Fluri, P., Imdorf, A. (1998) A look under the cap: the reproductive behaviour of Varroa in the capped brood of the honey bee. Am. Bee J. 138, 528–533. Duay, P., de Jong, D., Engels, W., 2002. Decreased flight performance and sperm

production in drones of the honey bee (Apis mellifera) slightly infested by Varroa destructor mites during pupal development. *Genet. Mol. Res*. 1, 227–232.

Gast, M. (2005). *802.11 wireless networks: the definitive guide*. “O’Reilly Media, Inc.".

Gould, J.L., Kirschvink, J.L., Deffeyes, K.S. (1978) Bees have magnetic remanence. *Science* 201, 1026–1028.

Headlee, T., & Burdette, R. (1929). Some Facts Relative to the Effect of High Frequency Radio Waves on Insect Activity. *Journal of the New York Entomological Society*, 37(1), 59-64.

Hsu, C. Y., & Li, C. W. (1993). The ultrastructure and formation of iron granules in the honeybee (Apis mellifera). *Journal of Experimental Biology*, *180*(1), 1-13.

Hsu, C.Y., Li, C.W. (1994) Magnetoreception in honeybees. *Science* 265, 95–97.

Hsu, C.Y., Ko, F.Y., Li, C.W., Fann, K., Lue, J.T. (2007) Magnetoreception system in honeybees (Apis mellifera). *PLoS. ONE* 2, e395.

Jassem, H.C. (2010). Municipal WiFi: The Coda. *Journal of Urban Technology*, 17(2), 3-20.

Johnson, R. (2007). Recent honey bee colony declines. LIBRARY OF CONGRESS WASHINGTON DC CONGRESSIONAL RESEARCH SERVICE.

Kumar, N. R., Sangwan, S., & Badotra, P. (2011). Exposure to cell phone radiations produces biochemical changes in worker honey bees. *Toxicology international*, 18(1), 70.

Liang, C. H., Chuang, C. L., Jiang, J. A., & Yang, E. C. (2016). Magnetic Sensing through the Abdomen of the Honey bee. *Scientific reports*, 6.

Lu, C., Warchol, K. M., & Callahan, R. A. (2014). Sub-lethal exposure to neonicotinoids impaired honey bees winterization before proceeding to colony collapse disorder. *Bulletin of Insectology*, *67*(1), 125-130.

Naug, D. (2009). Nutritional stress due to habitat loss may explain recent honeybee colony collapses. *Biological Conservation*, *142*(10), 2369-2372.

Oldroyd, B. P. (2007). What's killing American honey bees? *PLoS Biology* 5(168), e168.

Sainudeen, S. S. (2011). Impact of mobile phones on the density of honeybees. *Journal of Horticulture and Forestry*, 3(4), 131-133.

Texas A&M University - Agricultural Communications. (2006, December 29). Research Upsetting Some Notions About Honey Bees. *ScienceDaily*. Retrieved May 19, 2017 from www.sciencedaily.com/releases/2006/12/061211220927.htm

Appendix A: Instrumentation Settings

Instrumentation settings for the dynamic light scattering instrument, scanning electron microscope, mars 6 microwave digester and HP digital RF Signal generator.

Instrument	Material	Refractive Index (RI)	Absorption	Temperture (℃)	Cell Type	
DLS	Magnetite (Fe_3O_4)	2.42	0.5 @ 632.5 nm		Disposable cuvette	
	Water (H_2O) (Dispersant)	1.33		25	Disposable cuvette	
SEM	**Working distance (mm)**	**Accelerated Voltage (kV)**				
	10 - 15	15				
Mars 6 Microwave	**Stage**	**Temperature (℃)**	**Ramp (mm:ss)**	**Hold (mm:ss)**	**Pressure (PSI)**	**Power (Watts)**
	1	200	15:00	15:00	800	900-1050
Signal Generator	**Frequency (GHz)**	**Power Level (Watts)**	**Wave Type**			
	2.4	0.003	Modular			

Appendix B: DLS Data

Average particle size, standard deviation, number of runs, number of measurements and measurement angle for both preliminary data and full hive exposure DLS data.

Preliminary Data					
Sample #	**Average Particle size (nm)**	**Standard Deviation (nm)**	**Runs**	**Measurements**	**Measurement Angle**
Before	343.4	104.6	100	1	Dual (90° & 13°)
After	783.6	152	100	1	Dual (90° & 13°)
Non-Exposed					
Sample #	**Average Particle size (nm)**	**Standard Deviation (nm)**	**Runs**	**Measurements**	**Measurement Angle**
1	1200	87.27	60	1	Dual (90° & 13°)
2	1062	68.63	55	1	Dual (90° & 13°)
3	1215	84.91	100	1	Dual (90° & 13°)
4	952.9	100.2	73	1	Dual (90° & 13°)
5	1020	119.8	82	1	Dual (90° & 13°)
6	766.4	56.26	72	1	Dual (90° & 13°)
7	0	0	0	1	Dual (90° & 13°)
8	948.8	28.63	91	1	Dual (90° & 13°)
9	1265	50.21	100	1	Dual (90° & 13°)
10	841.1	75.12	5	1	Dual (90° & 13°)
11	948.6	28.91	41	1	Dual (90° & 13°)
12	736.5	73.49	100	1	Dual (90° & 13°)
13	867.6	62.19	100	1	Dual (90° & 13°)
14	646.2	56.2	100	1	Dual (90° & 13°)
15	1005	70.92	92	1	Dual (90° & 13°)
16	1105	13.87	100	1	Dual (90° & 13°)
17	1098	34.47	63	1	Dual (90° & 13°)
18	1198	87.36	7	1	Dual (90° & 13°)
19	1178	86.09	100	1	Dual (90° & 13°)
20	1074	62.3	42	1	Dual (90° & 13°)
21	1017	74.28	100	1	Dual (90° & 13°)
22	0	0	0	1	Dual (90° & 13°)
23	1040	74.91	63	1	Dual (90° & 13°)
24	1217	84.23	41	1	Dual (90° & 13°)
25	636.1	39.98	27	1	Dual (90° & 13°)
Exposed					
Sample #	**Average Partcle Size (nm)**	**Standard Deviation (nm)**	**Runs**	**Measurements**	**Measurement Angle**
1	1137	66.29	42	1	Dual (90° & 13°)
2	936.9	45.49	100	1	Dual (90° & 13°)
3	501.7	73.03	63	1	Dual (90° & 13°)
4	1243	72.35	8	1	Dual (90° & 13°)
5	1351	96.28	12	1	Dual (90° & 13°)
6	1157	90.92	100	1	Dual (90° & 13°)
7	1136	65.66	100	1	Dual (90° & 13°)
8	1072	65.84	100	1	Dual (90° & 13°)
9	1081	56.76	92	1	Dual (90° & 13°)
10	1063	68.53	34	1	Dual (90° & 13°)
11	898.3	64.7	63	1	Dual (90° & 13°)
12	614.4	69.4	74	1	Dual (90° & 13°)
13	1170	84.07	63	1	Dual (90° & 13°)
14	1173	85.58	100	1	Dual (90° & 13°)
15	1068	65.5	100	1	Dual (90° & 13°)
16	1127	55.76	90	1	Dual (90° & 13°)
17	1223	82.5	90	1	Dual (90° & 13°)
18	893.4	65.13	8	1	Dual (90° & 13°)
19	933	48.5	53	1	Dual (90° & 13°)
20	1052	72.47	100	1	Dual (90° & 13°)
21	1051	72.71	16	1	Dual (90° & 13°)
22	1119	45.71	100	1	Dual (90° & 13°)
23	1010	72.67	70	1	Dual (90° & 13°)
24	1011	72.71	75	1	Dual (90° & 13°)
25	1045	74.22	25	1	Dual (90° & 13°)